



Published in final edited form as:

Neurotoxicology. 2017 December ; 63: 57–69. doi:10.1016/j.neuro.2017.09.006.

Trace amine-associated receptor 1 regulation of methamphetamine-induced neurotoxicity

Nicholas B. Miner^{a,b}, Josh S. Elmore^c, Michael H. Baumann^c, Tamara J. Phillips^{a,b,d}, and Aaron Janowsky^{a,b,d,e,*}

^aResearch Service, VA Portland Health Care System, Portland, OR, USA

^bDepartment of Behavioral Neuroscience, Oregon Health & Science University, Portland, OR, USA

^cDesigner Drug Research Unit, Intramural Research Program, National Institute on Drug Abuse, National Institutes of Health, Baltimore, Maryland 21224, United States

^dThe Methamphetamine Abuse Research Center, Oregon Health & Science University, Portland, OR, USA

^eDepartment of Psychiatry, Oregon Health & Science University, Portland, OR, USA

Abstract

Trace amine-associated receptor 1 (TAAR1) is activated by methamphetamine (MA) and modulates dopaminergic (DA) function. Although DA dysregulation is the hallmark of MA-induced neurotoxicity leading to behavioral and cognitive deficits, the intermediary role of TAAR1 has yet to be characterized. To investigate TAAR1 regulation of MA-induced neurotoxicity, *Taar1* transgenic knock-out (KO) and wildtype (WT) mice were administered saline or a neurotoxic regimen of 4 i.p. injections, 2 hr apart, of MA (2.5, 5, or 10 mg/kg). Temperature data were recorded during the treatment day. Additionally, striatal tissue was collected 2 or 7 days following MA administration for analysis of DA, 3,4-dihydroxyphenylacetic acid (DOPAC), homovanillic acid (HVA), and tyrosine hydroxylase (TH) levels, as well as glial fibrillary acidic protein (GFAP) expression. MA elicited an acute hypothermic drop in body temperature in *Taar1*-WT mice, but not in *Taar1*-KO mice. Two days following treatment, DA and TH levels were lower in *Taar1*-KO mice compared to *Taar1*-WT mice, regardless of treatment, and were dose-dependently decreased by MA. GFAP expression was significantly increased by all doses of MA at both time points and greater in *Taar1*-KO compared to *Taar1*-WT mice receiving MA 2.5 or 5 mg/kg. Seven days later, DA levels were decreased in a similar pattern: DA was significantly lower in *Taar1*-KO compared to *Taar1*-WT mice receiving MA 2.5 or 5 mg/kg. TH levels were uniformly decreased by MA, regardless of genotype. These results indicate that activation of TAAR1 potentiates MA-induced

*Correspondence: Aaron Janowsky, Address: Research Service (RD-22), Veterans Affairs Medical Center, 3710 SW US Veterans Hospital Rd, Portland, OR 97239-3098, janowsky@ohsu.edu, Phone: 503-721-7912, Fax: 503-721-7839.

Conflicts of Interest

The authors do not have any conflicts of interest to declare.

Publisher's Disclaimer: This is a PDF file of an unedited manuscript that has been accepted for publication. As a service to our customers we are providing this early version of the manuscript. The manuscript will undergo copyediting, typesetting, and review of the resulting proof before it is published in its final citable form. Please note that during the production process errors may be discovered which could affect the content, and all legal disclaimers that apply to the journal pertain.

hypothermia and TAAR1 confers sustained neuroprotection dependent on its thermoregulatory effects.

Keywords

TAAR1; neurotoxicity; methamphetamine; temperature; dopamine; GFAP

1. Introduction

Methamphetamine (MA) abuse and addiction continue unabated. Worldwide, MA is the second most commonly used illicit drug, exceeded only by cannabis (United Nations Office on Drugs and Crime, 2016). The latest National Survey on Drug Use and Health reported 569,000 Americans used MA in the past month of 2014 (Center for Behavioral Health Statistics and Quality, 2015) and MA-related emergency room visits increased from 68,000 in 2007 to 103,000 in 2011 (Substance Abuse and Mental Health Services Administration, 2014). Beyond the detrimental effects of MA on physical health, such as increased cardiovascular and cerebrovascular pathologies (Darke *et al.*, 2008;Mooney *et al.*, 2009), the impact of neurotoxic effects of MA are manifold, including impaired information processing and memory, and increased impulsivity (Simon *et al.*, 2000;Hoffman *et al.*, 2006;Scott *et al.*, 2007), as well as increased likelihood of mental illnesses, such as anxiety, depression, and psychosis (McKetin *et al.*, 2006;Glasner-Edwards *et al.*, 2010). These neurotoxic effects are primarily attributed to the effects of MA on dopaminergic systems (Wilson *et al.*, 1996;Volkow *et al.*, 2001).

The trace amine-associated receptor 1 (TAAR1) is a G α_s -type protein-coupled receptor (GPCR) activated by endogenous trace amines, such as β -phenethylamine and tyramine. It is also activated by amphetamine-type substances, including MA and 3,4-methylenedioxymethamphetamine (MDMA) (Bunzow *et al.*, 2001;Borowsky *et al.*, 2001). Receptor stimulation increases cytosolic cyclic AMP, *via* adenylyl cyclase activation, and initiates protein kinase A and C (PKA and PKC) signaling cascades (Bunzow *et al.*, 2001;Panas *et al.*, 2012;Shi *et al.*, 2016). TAAR1 is expressed in numerous brain regions, and particularly in monoaminergic systems: substantia nigra, striatum, ventral tegmental area, nucleus accumbens, dorsal raphe nucleus, and locus coeruleus (Borowsky *et al.*, 2001;Lindemann *et al.*, 2008). The TAAR1 acts as a neuromodulator of dopamine (DA); activation inhibits DA neuron firing (Lindemann *et al.*, 2008;Revel *et al.*, 2011). These and additional findings suggest that TAAR1 plays a role in addiction to amphetamine-type drugs as well as a broader role in several other neuropsychiatric disorders (Wolinsky *et al.*, 2007;Sotnikova *et al.*, 2008;Revel *et al.*, 2013;Harmeier *et al.*, 2015). However, the potential role of TAAR1 in modulating MA-induced neurotoxicity has yet to be reported.

The neurotoxic effects of MA are attributed to alterations of the dopamine (DA) transporter (DAT) and vesicular monoamine transporter 2 (VMAT2) function. A substrate of DAT, MA reverses the normal direction of flux at the plasmalemmal transporter, resulting in increased extracellular levels of DA. Additionally, MA is internalized by DAT where it interacts as a substrate of VMAT2, inducing depletion of vesicular stores of DA and increasing cytosolic

levels of DA (Fleckenstein *et al.*, 2007;Krasnova & Cadet, 2009). A potent inhibitor of monoamine oxidase A, MA also impairs DA metabolism, exacerbating the elevated cytosolic DA concentration. As cytosolic DA levels rise, DA is auto-oxidized to form harmful DA quinones, which, along with reactive oxygen species (ROS), increase oxidative stress within the cell leading to DA terminal degeneration (Cubells *et al.*, 1994;LaVoie & Hastings, 1999). MA also increases striatal glutamate (GLU) levels leading to excitotoxicity and increased levels of ROS, contributing to terminal degeneration (Yamamoto & Raudensky, 2008). MA dose-dependently increases striatal DA terminal degeneration (Sonsalla *et al.*, 1989;Ares-Santos *et al.*, 2014;McConnell *et al.*, 2015), although the mesolimbic pathway is spared (Granado *et al.*, 2010;Kuhn *et al.*, 2011) and is characterized by a decrease in striatal DA markers: tyrosine hydroxylase (TH), the rate limiting enzyme for DA synthesis, DA and its metabolites 3,4-dihydroxyphenylacetic acid (DOPAC) and homovanillic acid (HVA), and DAT and VMAT2 levels (O'Callaghan & Miller, 1994;Guilarte *et al.*, 2003;Eyerman & Yamamoto, 2007). Striatal astrocyte activation, another robust marker of neurotoxicity, is characterized by expression of glial fibrillary acidic protein (GFAP) (O'Callaghan & Sriram, 2005). An early reaction to neuronal injury, a sustained increase in GFAP expression leads to increased ROS and is correlated with increased terminal degeneration (Fukumura *et al.*, 1998;Lau *et al.*, 2000;O'Callaghan *et al.*, 2014). These markers are frequently measured 2–3 days post-treatment to capture maximal effects (Fantegrossi *et al.*, 2008;Guillot *et al.*, 2008;Anneken *et al.*, 2015), but measurement at this time may only represent transient neurotoxicity. A second time point of 7 days was chosen as a reflection of sustained neurotoxicity. Under similar treatments and doses, DA, TH and GFAP remain significantly altered at 7, 14 and 21 days post-treatment (O'Callaghan & Miller, 1994;Ladenheim *et al.*, 2000;McConnell *et al.*, 2015). Although TH levels are still significantly decreased 30 days later, some recovery from peak depletion is observed (Ares-Santos *et al.*, 2014). Recovery at one month is more commonly investigated in rat models of neurotoxicity and demonstrates that DA and TH levels remain diminished (Morgan & Gibb, 1980;Hanson *et al.*, 2009).

While amphetamines are primarily associated with hyperthermia (Bowyer & Hanig, 2014;Matsumoto *et al.*, 2014), acute decreases in body temperature are observed when they are administered at normothermic and lower ambient temperatures (Bowyer *et al.*, 2001;Myles *et al.*, 2008;Shortall *et al.*, 2013) or at lower doses (Harkness *et al.*, 2015), and particularly when animals are singly housed (Fantegrossi *et al.*, 2008;Docherty & Green, 2010). Although MA-induced neurotoxicity is exacerbated by hyperthermia, (Bowyer *et al.*, 1994;Miller & O'Callaghan, 2003;Sharma *et al.*, 2015), neurotoxicity can still occur in its absence under the above conditions or when pharmacologically blocked (Albers & Sonsalla, 1995). We have previously demonstrated that a neurotoxic regimen of MDMA, administered in a normothermic environment, decreases striatal DA and TH levels, and increases GFAP expression, without eliciting hyperthermia, differentiating drug-dependent from hyperthermia-induced effects (Miner *et al.*, 2017). By studying MA without increasing body temperature above baseline, it is possible to isolate the neurotoxic effects of the drug, independent of synergistic effects of hyperthermia on neurotoxicity.

The *Taar1* transgenic knockout (KO) mouse model has previously been used to investigate the acute effects of stimulating TAAR1 with amphetamines. The KO and wild type (WT)

genotypes have similar baseline phenotypes: body weight, temperature, anxiety levels (elevated plus maze), working memory (Y-maze), locomotion (open field activity), and striatal levels of monoamines: DA, serotonin (5HT), and norepinephrine (NE) (Wolinsky *et al.*, 2007; Lindemann *et al.*, 2008), although there are some differences between genotypes. While striatal levels of monoamines are equivalent at baseline, basal DA levels in the nucleus accumbens (NAc) are increased in *Taar1*-KO mice compared to *Taar1*-WT (Leo *et al.*, 2014). Additionally, *Taar1*-KO mice over express D₂ receptors in the striatum along with an increased density of D₂ in high-affinity states for DA (D₂^{High}) compared to *Taar1*-WT mice (Wolinsky *et al.*, 2007; Espinoza *et al.*, 2015a). However, the most significant difference between the genotypes is sensitivity to various effects of MA, AMPH, and MDMA. In the absence of TAAR1, these drugs elicit increased DA, 5HT, and NE extracellular levels in the striatum, hyperdopaminergic firing, as well as increased locomotor activity, self-administration, conditioned place preference, and altered thermal response (Wolinsky *et al.*, 2007; Lindemann *et al.*, 2008; Di Cara *et al.*, 2011; Achat-Mendes *et al.*, 2012; Espinoza *et al.*, 2015a; Harkness *et al.*, 2015). As sensitivity to many of these effects is correlated with increased neurotoxicity (Fumagalli *et al.*, 1998; Zhang *et al.*, 2006; Kita *et al.*, 2009), we hypothesized that the absence of TAAR1 activation in *Taar1*-KO mice would increase MA-induced neurotoxicity compared to *Taar1*-WT mice.

While TAAR1 research has focused on the acute effects of single doses of amphetamines, the results presented here indicate a regulatory role for TAAR1 on the effects of a binge-like dosing regimen of MA, which persist up to 7 days later. Activation of TAAR1 elicited a hypothermic response to MA and decreased MA-induced neurotoxicity. For the first time, we demonstrate MA-induced neurotoxicity is increased in animals lacking TAAR1, indicating that activation of the receptor confers neuroprotection.

2. Material and methods

2.1 Drugs and chemicals

Racemic methamphetamine (MA) hydrochloride was generously provided by the National Institute on Drug Abuse (NIDA) Research Resources Drug Supply program (Bethesda, MD). The materials used in the TH and GFAP immunoassays have been described previously (O'Callaghan, 2002; Sriram *et al.*, 2004). All other reagents were obtained from standard commercial sources, unless otherwise noted.

2.2 *Taar1*-KO mouse breeding and genotyping

The *Taar1*-KO mice were obtained from the U.C. Davis Knockout Mouse Project (KOMP; www.komp.org) as previously described (Harkness *et al.*, 2015). Briefly, chimeric mice were created using C57BL/6N ES cells in which the entire *Taar1* coding region was deleted by homologous recombination, using the Veloci-Gene Null Allele Bac vector, and then injected into BALB/c blastocysts. The chimeras were bred with wild-type C57BL/6N mice and their offspring genotyped according to the strategy recommended by KOMP using the following primers: ACTCTTCACCAAGAATGTGG (forward); CCAACAGCGCTCAACAGTTC (reverse, wild-type allele); GTCGTCCTAGCTTCCTCACTG (reverse, null allele). Male and

female siblings, identified as heterozygous for the targeted locus, were subsequently bred to produce *Taar1*-WT and *Taar1*-KO littermates.

2.3 Animal maintenance and housing

Mice of both sexes were used in all studies (10 – 20 weeks old). Before experiment initiation, mice were group-housed in filtered acrylic plastic shoebox cages (28 cm×18 cm×13 cm; l×w×h), fitted with wire tops. Cages were lined with ECO-Fresh bedding (Absorption Corporation, Ferndale, WA). Mice had free access to rodent chow (5LOD, 5.0% fat content, Purina Mills, St. Louis, MO) and water *ad libitum*. Colony room temperature was 21±1°C and lights were maintained on a 12:12 hr light:dark schedule, with lights on at 0600 hr. Procedures were conducted in accordance with the National Institutes of Health (NIH) Guide for the Care and Use of Laboratory Animals, and were approved by the Veterans Affairs Portland Health Care System Institutional Animal Care and Use Committee.

2.4 Drug treatment and temperature recording

Two days prior to drug administration, mice were implanted with IPTT-300 temperature transponders (BioMedic Data Systems, Seaford, DE) to assess body temperature via telemetry. Animals were anesthetized with isoflurane (5% induction, 2.5% maintenance) and transponders were subcutaneously injected dorsally between the shoulders. On the day of drug administration, animals were weighed (Mean = 26.1 g, SEM = 0.4 g) and transferred from group to individual housing. After a 1-hr acclimation period, each animal received four i.p. injections (2 hr apart) of saline or MA (2.5, 5, or 10 mg/kg). MA was dissolved in 0.9% saline and injected in a final volume of 10 ml/kg. Temperature recording began immediately prior to the first drug administration to establish baseline and was subsequently measured every 15 min for 8 hr. Temperatures were non-invasively recorded using the DAS-8001 reader console and smart probe from BioMedic Data Systems. An animal was removed from the cage, the smart probe was placed within 5 cm of the embedded transponder to acquire a temperature reading, and then the mouse was returned to the cage. The ambient temperature of the testing environment was 23 ± 1°C, a normothermic temperature at which neurotoxicity still occurs (Ali *et al.*, 1996; Miller & O'Callaghan, 2003; Granado *et al.*, 2011). Mice were euthanized by cervical dislocation followed by decapitation, 2 or 7 days after the final saline or MA treatment. The striatum was removed, flash-frozen, and stored at -70°C until time of assay. Striatal tissue from each animal was dissected and each half was used for either monoamine and metabolite analyses or TH and GFAP assays (counterbalanced by side of brain).

2.5 Quantification of monoamines and metabolite levels

Striatal DA, DOPAC, HVA, 5HT, 5HIAA, and NE were quantified *via* high-performance liquid chromatography with electrochemical detection (HPLC-ECD). Tissue samples were weighed, homogenized in 0.1N HClO₄, and centrifuged at 16,600g for 18 min at 4°C. Concentrations of monoamines and their metabolites were quantified in the supernatant using HPLC-ECD. Aliquots were injected onto an HPLC column linked to a coulometric detector (ESA Model Coulochem III, Dionex, Chelmsford, MA). Mobile phase consisting of 50 mM sodium phosphate monobasic, 250 μM Na₂EDTA, 0.03% sodium octane sulfonic

acid, and 25% methanol (pH = 2.75) was recirculated at 0.9 ml/min. Data were acquired by a Waters Empower software system, where peak heights of unknowns were compared with those of standards. The lower limit of assay sensitivity (3 x baseline noise) was 1 pg/20 μ l sample.

2.6 Quantification of tyrosine hydroxylase levels

Tissue was prepared as previously outlined (O'Callaghan, 2002; Miller & O'Callaghan, 2003; Granado *et al.*, 2011). Striatal tissue was homogenized in 10 volumes of 1% hot (85–95°C) sodium dodecyl sulfate (SDS) by sonification and total protein concentration determined by BCA assay. TH holoenzyme protein was assessed using a previously published ELISA with minor modifications (Sriram *et al.*, 2004). In brief, an anti-TH monoclonal mouse antibody (1:500; Santa Cruz Biotechnology, Dallas, TX) was coated on the wells of Nunc MaxiSorp microplates (Thermo Fisher Scientific, Waltham, MA). The SDS homogenates and standards (prepared from control mouse striatum) were diluted in phosphate-buffered saline (pH = 7.4) containing 0.5% Triton X-100. After blocking non-specific binding with 5% non-fat dry milk, aliquots of the homogenate and standards were added to the wells in duplicate and incubated. Following washes, an anti-TH polyclonal rabbit antibody (1:500; EMD Millipore, Billerica, MA) was added to 'sandwich' the TH protein between the two antibodies, coupled with a horseradish peroxidase (HRP) conjugated secondary anti-rabbit IgG antibody (1:3000; Santa Cruz Biotechnology, Dallas, TX). Peroxidase activity was detected using the substrate tetramethylbenzidine (Sigma-Aldrich, St. Louis, MO), followed by addition of a 1N sulfuric acid stop solution. Quantification was performed by measuring absorbance with a microplate reader (BIO-RAD Laboratories, Hercules, CA), at 450 nm. The amount of TH in the samples was calculated and expressed as TH (μ g) per total protein (mg) loaded.

2.7 Quantification of GFAP expression

The same tissue homogenate used for TH analysis was also used for the GFAP assay. Striatal GFAP levels were quantified using a similar ELISA protocol (O'Callaghan, 2002) as described for TH quantification, with the following differences: an anti-GFAP polyclonal rabbit antibody (1:400; DAKO, Carpinteria, CA) was used as the capture antibody and an anti-GFAP monoclonal mouse antibody (1:250; EMD Millipore-Calbiochem, Billerica, MA) was used as the detection antibody coupled with a secondary anti-mouse IgG-HRP antibody (1:3000; Santa Cruz Biotechnology, Dallas, TX).

2.8 Data analysis

Biochemical data were analyzed by three-way analysis of variance (ANOVA) with sex, genotype, and dose as between-group factors, at each time point, independently. Temperature data were analyzed using a repeated measures four-way ANOVA with time as a within-subject factor and sex, genotype, and dose as between-group factors. As there were no significant interactions involving sex in initial analyses, this factor was excluded from further analyses. Significant two-way interactions were further investigated using simple main effect analyses and/or *post hoc* mean comparisons using the Newman-Keuls test, when appropriate. For temperature data, subsequent analyses were conducted at 30 min after each injection as, under the described conditions, the maximum hypothermic drop occurs 30 min

following administration of MA or MDMA (Harkness *et al.*, 2015; Miner *et al.*, 2017). Data were analyzed for outliers using Dixon's Q-test at 90% confidence. All statistical analyses were performed using Statistica version 13 software (StatSoft Inc., Tulsa, OK). Differences were considered significant at $p < 0.05$.

3. Results

3.1 Thermoregulation

Prior to the first injection, the mean baseline temperature of all animals was 38.3°C (SEM = 0.03°C), with no significant between-genotype or -group differences. Profound genotype-dependent MA-induced hypothermia was observed. MA did not elicit hyperthermia, defined as a 0.5°C increase in body temperature above the temperature of the untreated animal, in any group. Temperature data (Fig. 1), analyzed using a three-way repeated measures ANOVA, revealed a significant genotype x dose x time interaction ($F_{96, 4288} = 4.9, p < 0.0001$). There was no difference in temperature between genotypes for mice receiving saline (Fig. 1A), although there was a main effect of time ($F_{32, 1312} = 1.3, p < 0.0001$) as temperatures in these control groups decreased over the 8 hr period, likely attributable to single housing.

Examination of the effects of each dose of MA revealed significant genotype x time interactions for all 3 doses: MA 2.5 mg/kg ($F_{32, 672} = 9.4, p < 0.0001$) (Fig. 1B), MA 5 mg/kg ($F_{32, 1120} = 15.3, p < 0.0001$) (Fig. 1C), and MA 10 mg/kg ($F_{32, 1184} = 4.0, p < 0.0001$) (Fig. 1D). Analyses of genotype differences were conducted within each dose of MA using simple main effect analyses at each 30 min post-injection time point to investigate the hypothermic drop in body temperature. The temperatures of *Taar1*-WT mice receiving MA 2.5 mg/kg were significantly lower 30 min after each of the four MA injections compared to their *Taar1*-KO counterparts, whereas *Taar1*-WT mice administered either MA 5 or 10 mg/kg had significantly lower temperatures than *Taar1*-KO mice after the first three injections.

Next, examination of the data for each genotype revealed a significant dose x time interaction for both genotypes: *Taar1*-WT ($F_{96, 2208} = 10.8, p < 0.0001$) and *Taar1*-KO ($F_{96, 2080} = 7.5, p < 0.0001$). Simple main effects analysis was then used to statistically investigate MA effects within each genotype at the 30 min post-injection time points. There was a significant effect of dose after the first, second and third injections in *Taar1*-WT mice (all $p < 0.0001$) and after the first and fourth injections in *Taar1*-KO mice (both $p < 0.001$ and $p < 0.01$). Newman-Keuls *post hoc* mean comparisons indicated that 30 min following the first and second injection *Taar1*-WT mice treated with all MA doses had lower body temperatures than *Taar1*-WT mice receiving saline (Table 1). Thirty min after the third injection, the difference was significant in *Taar1*-WT mice receiving MA 2.5 or 5 mg/kg, but not 10 mg/kg, and there were no significant effects of MA 30 min after the fourth injection. In *Taar1*-KO mice, body temperature was significantly reduced by MA 5 and 10 mg/kg 30 min after the first injection. There were no other significant hypothermic responses to MA in *Taar1*-KO mice, though body temperature was significantly increased 30 min following the fourth injection in mice receiving MA 2.5 mg/kg. However, this increase of 0.8°C for *Taar1*-KO mice at this dose and time resulted in a mean body temperature of 38.5°C compared to

the initial basal temperature of 38.3°C, providing little evidence of MA-induced hyperthermia.

3.2 Monoamines and metabolite levels

MA dose-dependently decreased striatal levels of DA and DOPAC at both time points (2 and 7 days following the final injection) and HVA at 2 days (Fig. 2). Seven days later, levels of DA were lower in *Taar1*-KO mice compared to *Taar1*-WT mice after MA 2.5 and 5 mg/kg, but not 10 mg/kg, while DOPAC and HVA were lower in *Taar1*-KO mice compared to *Taar1*-WT mice, regardless of treatment. DA turnover rates (calculated by dividing DOPAC levels by DA) at both 2 and 7 days following the final treatment were higher in *Taar1*-KO compared to *Taar1*-WT mice, regardless of treatment. These characterizations are supported by the following statistical results. At 2 days following the final administration of saline or MA, a two-way ANOVA for DA level data identified a main effect of genotype ($F_{1,62} = 17.16$, $p < 0.001$) and dose ($F_{3,62} = 32.78$, $p < 0.0001$), but no significant interaction (Fig. 2A). DA levels were lower in *Taar1*-KO mice compared to *Taar1*-WT mice, regardless of treatment, and all doses of MA significantly decreased DA levels compared to saline-treated animals, regardless of genotype. At 7 days after saline or MA administration, there was a significant genotype x dose interaction ($F_{3,61} = 3.04$, $p < 0.05$) (Fig. 2B). Simple main effect analysis of the effect of genotype at each dose revealed no difference between genotypes for saline-treated animals, but *Taar1*-KO mice receiving either MA 2.5 or 5 mg/kg had significantly lower levels of striatal DA in comparison to *Taar1*-WT mice. There was no difference between genotypes at MA 10 mg/kg. Simple main effect analysis of the effect of dose within each genotype indicated significant dose-dependent effects in both *Taar1*-WT ($p < 0.0001$) and *Taar1*-KO ($p < 0.0001$) mice. In *Taar1*-WT mice, Newman-Keuls *post hoc* mean comparisons indicated that DA levels were significantly decreased by the MA 5 and 10 mg/kg doses compared to saline-treated animals, but not by MA 2.5 mg/kg. In *Taar1*-KO mice, DA levels were significantly decreased by all three MA doses compared to saline-treated animals.

Two days after the final administration of saline or MA, a two-way ANOVA for DOPAC level data revealed only a main effect of dose ($F_{3,62} = 12.94$, $p < 0.0001$) (Fig. 2C). DOPAC levels were significantly decreased by MA 5 and 10 mg/kg, but not 2.5 mg/kg, compared to saline-treated animals, regardless of genotype. At 7 days after MA administration, there was a main effect of genotype ($F_{1,61} = 13.43$, $p < 0.001$) and dose ($F_{3,61} = 35.34$, $p < 0.0001$), but no significant genotype x dose interaction (Fig. 2D). DOPAC levels were lower in *Taar1*-KO mice compared to *Taar1*-WT mice, regardless of treatment. Only the two higher doses of MA significantly decreased DOPAC levels compared to saline-treated animals, regardless of genotype.

There were no significant effects on HVA levels 2 days following the final administration of MA (Fig. 2E), but 7 days later there was a main effect of genotype ($F_{1,61} = 5.76$, $p < 0.05$) and dose ($F_{3,61} = 22.03$, $p < 0.0001$), though no significant interaction (Fig. 2F). HVA levels were lower in *Taar1*-KO mice compared to *Taar1*-WT mice, regardless of treatment. HVA levels were significantly increased by MA 2.5 mg/kg, but decreased by MA 5 and 10 mg/kg, in comparison to saline-treated animals, regardless of genotype.

At 2 days following the final injection of saline or MA, a two-way ANOVA for DA turnover data (expressed as a ratio of DOPAC/DA levels) identified a main effect of genotype ($F_{1,62} = 8.83$, $p < 0.01$) and dose ($F_{3,62} = 4.16$, $p < 0.01$), but no significant interaction (Fig. 2G). DA turnover was higher in *Taar1*-KO mice compared to *Taar1*-WT mice, regardless of treatment, and only MA 2.5 mg/kg significantly increased DA turnover compared to saline-treated animals, regardless of genotype. Seven days after the final administration of saline or MA, a two-way ANOVA for DA turnover data also found a main effect of genotype ($F_{1,61} = 12.30$, $p < 0.001$) and dose ($F_{3,61} = 20.09$, $p < 0.0001$), but no interaction (Fig. 2H). DA turnover was again higher in *Taar1*-KO mice compared to *Taar1*-WT mice, regardless of treatment, and only MA 10 mg/kg significantly increased DA turnover compared to saline-treated animals, regardless of genotype.

There were no significant interactions or main effects of genotype at 2 or 7 days following MA administration for 5HT, 5HIAA, 5HT turnover, or NE (Fig. 3). A two-way ANOVA revealed a main effect of dose for 5HT levels both 2 days ($F_{3,62} = 7.34$, $p < 0.001$) and 7 days ($F_{3,61} = 13.14$, $p < 0.0001$) following the final treatment (Fig. 3A and B). Two days following administration, 5HT levels were significantly decreased by MA 5 and 10 mg/kg compared to saline-treated animals, whereas 7 days after administration MA 2.5 mg/kg significantly increased 5HT levels compared to saline-treated animals, regardless of genotype. There were no significant main effects for 5HIAA (Fig. 3C and D) or 5HT turnover (5HIAA/5HT levels) (Fig. 3E and F). A two-way ANOVA identified a main effect of dose for NE levels both 2 days ($F_{3,62} = 4.06$, $p < 0.01$) and 7 days ($F_{3,61} = 4.88$, $p < 0.01$) after the last treatment of saline or MA (Fig. 3G and H). Two days following administration, NE levels were significantly decreased by MA 10 mg/kg compared to saline-treated animals, whereas 7 days following administration, MA 5 and 10 mg/kg significantly decreased NE levels compared to saline-treated animals, regardless of genotype.

3.3 Tyrosine hydroxylase levels

Overall, MA decreased striatal TH levels at each time point (2 and 7 days following final injection) and dose (2.5, 5, and 10 mg/kg). TH levels were also lower in *Taar1*-KO mice compared to *Taar1*-WT mice 2 days, but not 7 days, following final administration of saline or MA (Fig. 4). These characterizations are supported by the following statistical results. At 2 days following the final administration of saline or MA, a two-way ANOVA revealed a main effect of genotype ($F_{1,65} = 13.22$, $p < 0.001$) and dose ($F_{3,65} = 25.34$, $p < 0.0001$), but no significant interaction (Fig. 4A). TH levels were lower in *Taar1*-KO mice compared to *Taar1*-WT mice, regardless of treatment, and the two higher doses of MA (5 and 10 mg/kg), but not the 2.5 mg/kg dose, significantly decreased TH levels compared to saline-treated animals, regardless of genotype. At 7 days after MA administration, a two-way ANOVA revealed only a main effect of dose ($F_{3,59} = 25.12$, $p < 0.0001$) (Fig. 4B); all doses of MA decreased TH levels compared to levels in tissue from saline-treated controls, regardless of genotype.

3.4 GFAP expression

Overall, at both 2 and 7 days post MA administration, and at all doses (2.5, 5, or 10 mg/kg), MA increased striatal GFAP expression. GFAP was increased to a greater extent in striatal

tissue from *Taar1*-KO compared to *Taar1*-WT mice by both the MA 2.5 and 5 mg/kg doses (Fig. 5). These characterizations are supported by the following statistical results. At 2 days following the final administration of saline or MA, a two-way ANOVA revealed a significant genotype x dose interaction ($F_{3,36} = 4.17, p < 0.01$) (Fig. 5A). Simple main effect analysis of genotype at each dose revealed no difference between genotypes for saline-treated animals, but *Taar1*-KO mice receiving either MA 2.5 or 5 mg/kg expressed significantly higher levels of striatal GFAP in comparison to *Taar1*-WT mice ($p < 0.01$ for both doses). There was no difference between genotypes at MA 10 mg/kg. Simple main effect analysis of the effect of dose within each genotype indicated significant dose-dependent effects in both *Taar1*-WT ($p < 0.0001$) and *Taar1*-KO ($p < 0.0001$) mice. Newman-Keuls *post hoc* comparisons indicated all 3 doses of MA significantly increased levels of GFAP in both *Taar1*-WT and *Taar1*-KO mice compared to levels in saline-treated animals.

Similar results were obtained for striatal GFAP assessed 7 days after treatment. A two-way ANOVA revealed a significant genotype x dose interaction ($F_{3,58} = 5.38, p < 0.01$) (Fig. 5B). Again, simple main effect analyses of genotype at each dose revealed no difference between saline-treated *Taar1*-WT and -KO animals, but *Taar1*-KO mice receiving MA 2.5 or 5 mg/kg expressed significantly higher levels of GFAP than *Taar1*-WT mice, whereas there was no difference between genotypes administered the highest dose of MA. Simple main effect analysis of the effect of dose within each genotype indicated significant dose-dependent effects in both *Taar1*-WT ($p < 0.0001$) and *Taar1*-KO ($p < 0.0001$) mice. Newman-Keuls *post hoc* mean comparisons revealed that GFAP expression in *Taar1*-WT mice was only significantly elevated in mice treated with MA 5 mg/kg and 10 mg/kg compared to saline-treated animals, but all three doses of MA elevated GFAP expression in *Taar1*-KO mice compared to saline-treated mice.

4. Discussion

In this study we report for the first time that activation of TAAR1 by a binge-like regimen of MA altered thermoregulation and decreased markers of neurotoxicity both 2 and 7 days following administration. Activation of TAAR1 inhibits DA firing in the striatum, the locus of MA-induced neurotoxicity, and mice lacking TAAR1 have altered sensitivity to the acute effects of amphetamines, biochemically and behaviorally (Lindemann *et al.*, 2008;Revel *et al.*, 2011;Harkness *et al.*, 2015). Based on these findings, we administered MA to *Taar1*-WT and *Taar1*-KO mice and measured acute thermal response, as well as transient and sustained effects of MA on markers of DA terminal degeneration and astrogliosis.

The temperature findings present a novel insight into the effects of TAAR1 on thermoregulation and regulation of MA-induced neurotoxicity. MA elicited hypothermia in *Taar1*-WT, but not *Taar1*-KO mice. In *Taar1*-WT mice, hypothermia was inversely dose-dependent: the largest change in temperature and longest persisting effects were elicited by the two lower doses of MA, whereas hypothermia and genotype differences were attenuated at the highest dose. In *Taar1*-KO mice, MA elicited only mild fluctuations from the initial basal temperature. These findings indicate the hypothermic response to MA is dependent on activation of TAAR1. Direct stimulation of TAAR1, using the selective agonist RO5166017, has produced differing results: in C57BL/6 mice, a single dose of 1 mg/kg induced

hypothermia 45 min later (Revel *et al.*, 2011), while in Sprague-Dawley rats, doses of 3.2 – 10 mg/kg did not alter body temperature one hour post-injection (Siemian *et al.*, 2017). It is unclear whether this is a species and/or dose dependent effect. Although previous TAAR1 research on amphetamines support our finding of TAAR1-dependent MA-induced hypothermia (Di Cara *et al.*, 2011; Harkness *et al.*, 2015), Panas et al. (2010) found no difference between *Taar1*-WT and -KO mice in their thermal response to MA or MDMA. However, hypothermia was also absent and it is possible that under the reported conditions the drugs increased temperatures to a degree that masked the thermoregulatory effects of TAAR1. This masking theory is supported by the pattern in our data: as MA dose and number of injections increased, thermal response differences between genotypes dissipated. This indicates the hypothermic response to MA is superseded by non-TAAR1 mediated thermoregulatory mechanisms once a threshold of MA is reached. This is also the first study to investigate TAAR1 modulation of thermoregulation using multiple doses of MA to measure aggregate effects.

MA did not induce hyperthermia in animals of either genotype. When studying MA-induced neurotoxicity, hyperthermia can confound the ability to distinguish neurotoxicity attributable to the direct actions of MA versus the indirect effects of inducing hyperthermia, which leads to increased ROS production and permeability of the blood brain barrier (Kiyatkin & Sharma, 2009; Bowyer & Hanig, 2014). As body temperatures only reached a maximum increase of 0.2°C from the initial baseline temperature, the increase in MA-induced markers of neurotoxicity in *Taar1*-KO mice cannot be attributed to hyperthermic effects. Conversely, hypothermia can confer neuroprotection against MA. Typically, this is induced by lowering the ambient temperature to 15° or 4°C or by leveraging pharmacological agents to decrease temperature (Miller & O'Callaghan, 1994; Albers & Sonsalla, 1995; Ali *et al.*, 1996; Metzger *et al.*, 2000; Sharma *et al.*, 2015), whereas in the current study all animals received the same drugs under the same conditions. Therefore, it is possible that the increased MA-induced neurotoxicity in *Taar1*-KO mice is attributable to the absence of MA-induced hypothermia. This theory is supported by the connection between temperature data and neurotoxicity with regard to dose. Significant differences between genotypes in DA levels and GFAP expression occurred only at the two lower doses of MA, correlating with the greatest hypothermic responses.

At 2 days post-treatment, DA and TH levels were dose-dependently diminished and levels were lower when TAAR1 was absent, regardless of treatment. However, this should not be interpreted as differences in basal levels as 7 days following treatment there was no significant difference in saline-treated animals. The findings from 7 days post-treatment indicate sustained MA-induced decreases in DA levels are dose-dependently diminished when TAAR1 is activated: the lowest dose of MA did not decrease DA levels when TAAR1 was activated, but did when TAAR1 was absent; the middle MA dose (5mg/kg) further decreased DA levels when TAAR1 was not activated; and the highest dose of MA did not differentially decrease DA when the receptor was activated or not. However, TH levels were not differentially affected across genotype at this later timepoint, indicating activation of TAAR1 transiently altered TH levels, but the effects were not sustained. The difference in levels of DA and metabolites between genotypes coupled with equally diminished TH levels at this time point suggests the sustained effects of TAAR1 activation take place post-DA

synthesis. Although amphetamines acutely increase striatal levels of 5HT and NE, measured by microdialysis, in *Taar1*-KO compared to *Taar1*-WT mice (Lindemann *et al.*, 2008; Di Cara *et al.*, 2011), here there were no significant differences in striatal levels of 5HT, 5HIAA, or NE between genotypes 2 or 7 days following MA administration. This indicates that, while TAAR1 modulates acute MA-induced release of 5HT and NE, the modulatory effects of the receptor on striatal monoamine levels at later time points are DA specific, reflective of the selectivity of MA for DA terminal degeneration in mice (Krasnova & Cadet, 2009).

Astrocyte activation, a glial reaction to neuronal injury, is an established marker of MA-induced neurotoxicity. An increase in GFAP expression peaks 2–3 days after MA administration and correlates with increased neurotoxicity, inflammatory response, and ROS (O’Callaghan & Miller, 1994; Lau *et al.*, 2000; McConnell *et al.*, 2015), though it can also increase independently of decreases in markers such as TH and DA (Pu & Vorhees, 1993; Miner *et al.*, 2017). We report the novel finding that astrocyte activation in response to MA is increased when TAAR1 is not activated. At both time points, the two lower doses of MA increased GFAP expression in *Taar1*-KO compared to *Taar1*-WT mice (though not at the highest dose). Additionally, at 7 days following the last administration, the lowest dose of MA significantly increased GFAP expression in *Taar1*-KO mice compared to saline-treated mice, while there was no significant increase when TAAR1 was activated in *Taar1*-WT mice. This corresponds with the DA data, indicating activation of TAAR1 is neuroprotective at lower doses, but the effect is suppressed at the highest dose of MA.

When using a binge-like regimen in a mouse model, MA 10 mg/kg is a common dose based on its strong neurotoxic effects (O’Callaghan & Miller, 1994; Zhu *et al.*, 2006; Fantegrossi *et al.*, 2008; Grace *et al.*, 2010). In our experiments, this dose caused the largest changes in DA, TH, and GFAP, but abolished differences between genotypes. Comparing the two lower doses of MA, decreases in DA and TH levels were less than two-fold in *Taar1*-WT mice, though DA and TH levels were decreased more than two-fold in *Taar1*-KO mice receiving MA 5 mg/kg, indicating increased neurotoxicity. At peak astrocyte activation (2 days post-administration), increases in GFAP expression were even larger with MA 2.5 and 5 mg/kg increasing GFAP expression greater than two-fold in *Taar1*-WT mice and three-fold in *Taar1*-KO mice. This magnitude of change is commensurate with previous research using MA doses less than 10 mg/kg (Thomas *et al.*, 2004; McConnell *et al.*, 2015) and indicates that TAAR1 may play an even more significant role in astroglial activation than DA terminal degeneration.

The most likely explanation for the increase in MA-induced neurotoxicity in *Taar1*-KO mice is their lack of hypothermic response. However, it is possible that the neuroprotective and thermoregulatory effects of TAAR1 activation occur in tandem or independently. The intent of this study was to separate the hyperthermic influence from drug-dependent effects to better understand the effect of TAAR1 on both drug-related thermoregulation and neurotoxicity. However, studies are needed to determine whether the activation of TAAR1 diminishes MA-induced neurotoxicity due to its hypothermic effects or other mechanisms, potentially through pharmacologically equalizing temperature fluctuations. Additional

research is also warranted under environmental conditions where hyperthermia occurs to further explore TAAR1 regulation of temperature and MA-induced neurotoxicity.

While the effects of TAAR1 activation on the DA system are complex and its mechanism still not fully understood, significant attention has been focused on the D₂ receptor. Compared to *Taar1*-WT mice, *Taar1*-KO mice over-express D₂ receptors, possess increased density of D₂ in high-affinity states for DA (D₂^{High}), and express super-sensitivity to activation of post-synaptic D₂ receptors (Wolinsky *et al.*, 2007; Espinoza *et al.*, 2015a), traits associated with increased behavioral sensitivity to amphetamines (Seeman *et al.*, 2005; Shuto *et al.*, 2008). Additionally, inhibition of TAAR1 increases potency of D₂ agonists and reduces D₂ receptor desensitization rates (Bradaia *et al.*, 2009). Finally, TAAR1 and D₂ can form a heterodimer and the D₂ antagonist raclopride increases TAAR1 activation (Espinoza *et al.*, 2011). MA-induced neurotoxicity is D₂-mediated and D₂ antagonists, such as raclopride and eticlopride, diminish MA-induced neurotoxicity (DA, TH, DAT levels, and GFAP expression) and attenuate MA-induced hyperthermia (Albers & Sonsalla, 1995; Broening *et al.*, 2005; Xu *et al.*, 2005; Hadlock *et al.*, 2010). These markers of neurotoxicity are also lower in D₂-KO mice receiving MA, which exhibit MA-induced hypothermia as well, in comparison to D₂-WT mice (Granado *et al.*, 2011). It is possible that the absence of MA-induced hypothermia and increased neurotoxicity in *Taar1*-KO mice can be attributed to increased D₂ activation compared to when TAAR1 is activated in *Taar1*-WT mice. Future research on the intersection of TAAR1 and D₂ effects on MA-induced neurotoxicity are warranted. Additionally, as neurotoxicity is primarily attributed to increased cytosolic levels of DA (Fleckenstein *et al.*, 2007) and TAAR1 is predominantly localized intracellularly (Borowsky *et al.*, 2001), future research of TAAR1 regulation of MA-induced neurotoxicity could investigate acute intracellular markers of neurotoxicity, such as impaired VMAT2 expression and function (Fumagalli *et al.*, 1999; Guillot *et al.*, 2008), and increased DA quinone and ROS production (Cubells *et al.*, 1994; LaVoie & Hastings, 1999; Yamamoto & Raudensky, 2008).

TAAR1 mediation of excitotoxicity is another potential contributor to MA-induced neurotoxicity. The expression and phosphorylation of the GluN1 subunit of the N-methyl-D-aspartate (NMDA) glutamate receptors, in both the striatum and the prefrontal cortex (PFC), is lower in *Taar1*-KO mice compared to *Taar1*-WT mice (Espinoza *et al.*, 2015b; Sukhanov *et al.*, 2016). However, when amphetamine is administered, striatal expression and phosphorylation of GluN1 are increased only in *Taar1*-KO mice. This suggests amphetamines elicit an increased GLU response when TAAR1 is not activated, potentially contributing to increased neurotoxicity. Supporting a GLU system regulatory role for TAAR1, another study, using 6-hydroxydopamine (6-OHDA) to induce an animal model of Parkinson's disease, found the intra-striatal application of the selective TAAR1 agonist, RO5166017, blocked 6-OHDA-induced increased striatal GLU release (Alvarsson *et al.*, 2015). This same study also evaluated the effects of intra-striatal administration of 6-OHDA on DA markers using the *Taar1*-KO mouse model. Surprisingly, four weeks following 6-OHDA treatment, *Taar1*-WT mice had lower levels of striatal TH and DAT compared to *Taar1*-KO mice. While counter to our findings that activation of TAAR1 is neuroprotective against MA-induced neurotoxicity, it is important to note 6-OHDA lesioning destroys cell bodies in the substantia nigra pars compacta (SNpc) as well as terminals in the striatum

(Bove & Perier, 2012). Although there is evidence MA causes DA cell body death in the SNpc, MA primarily causes degeneration of striatal neuron terminals (Sonsalla *et al.*, 1996; Ares-Santos *et al.*, 2014). It is plausible TAAR1 has different modulatory roles in these two models of neuronal injury, as they differ in underlying mechanism, time course, and severity.

Astrocytes also decrease excitotoxicity *via* clearance of synaptic GLU by the excitatory amino acid transporter 2 (EAAT2) (Anderson & Swanson, 2000). Cisneros and Ghorpade (2014) investigated TAAR1 regulation of this function using cultured astrocytes. The authors found that knockdown of TAAR1 using RNA interference mitigates MA-induced downregulation of EAAT2 and increases GLU clearance, while overexpression of TAAR1 increases MA-induced EAAT2 downregulation and decreases GLU clearance. These findings imply MA activation of TAAR1 increases excitotoxicity, acting as a contributing factor to neurotoxicity (Burrows & Meshul, 1997). It is possible that MA activation of TAAR1 impairs astrocytic GLU function *in vitro*, but this effect is overshadowed by the increase in MA-induced astrocyte activation in *Taar1*-KO mice compared to *Taar1*-WT mice under physiological conditions. Additional research is warranted to explore TAAR1 regulation of other markers of gliosis, namely microglia. MA induces neuroinflammation and microgliosis, other contributors to neurotoxicity, through the production of harmful cytokines and chemokines, which is also ameliorated at lower temperatures (Thomas *et al.*, 2004; LaVoie *et al.*, 2004; O'Callaghan *et al.*, 2014).

Besides the *Taar1*-KO mouse model, mice selectively bred for MA consumption provide an alternative model for studying TAAR1. Initially developed as an animal model of differential genetic risk for MA intake, mice were bidirectionally selectively bred for voluntary MA consumption from the F2 cross of C57BL/6J (B6) and DBA2/J (D2) mice, using a two-bottle choice task, generating the MA high drinking (MAHDR) and MA low drinking (MALDR) lines (Wheeler *et al.*, 2009). It was later discovered that D2 mice possess a non-synonymous single-nucleotide polymorphism (SNP) that encodes a present, but non-functional TAAR1 and MAHDR mice were homozygous for the D2 allele, whereas MALDR mice were either hetero- or homozygous for the dominant B6 allele that encodes a functional TAAR1 (Harkness *et al.*, 2015; Shabani *et al.*, 2016). Besides differential MA consumption, MAHDR mice expressing the non-functional D2 *Taar1* allele exhibit MA-conditioned place preference (CPP), but are insensitive to MA-conditioned taste aversion (CTA), whereas MALDR mice expressing the functional B6 allele lack MA-induced CPP and exhibit high sensitivity to MA-induced CTA (Wheeler *et al.*, 2009; Shabani *et al.*, 2012). The selected lines are also similar to the *Taar1*-KO model in thermal response to MA: MALDR mice, similar to *Taar1*-WT, exhibit acute hypothermia in response to MA, whereas this response is mitigated in MAHDR mice, similar to *Taar1*-KO mice (Harkness *et al.*, 2015). The convergent results from the different TAAR1 animal models provide support for future use of both models to study TAAR1. This is particularly relevant as recent research has identified several synonymous and non-synonymous single nucleotide polymorphisms (SNP) in the human *Taar1* gene that can result in an expressed, but either sub- or non-functioning receptor (Shi *et al.*, 2016). From an epidemiological standpoint, this could identify a subset of the population at greater risk of physical and cognitive harm resulting from increased MA-induced neurotoxicity due to decreased TAAR1 activation. Additionally,

based on its neuroprotective qualities, TAAR1 agonists could prove a fruitful avenue for future research and development of pharmacological therapies to ameliorate the harmful impact of MA and possibly other DA neurotoxins in active or recovering addicts.

5. Conclusions

Our findings demonstrate for the first time that activation of TAAR1 potentiates MA-induced hypothermia and confers neuroprotection against MA-induced neurotoxicity with sustained effects up to a week following drug administration. Hypothermia in response to MA was only present in *Taar1*-WT mice and absent in *Taar1*-KO mice. MA-induced decreases in striatal DA levels and astrogliosis were diminished when TAAR1 was activated, but only by the lower doses of MA, corresponding with the greatest hypothermic responses. The hypothermic response in *Taar1*-WT mice was attenuated at the highest dose of MA and differences between genotypes in markers of neurotoxicity disappeared at this dose. These findings indicate the neuroprotection provided by TAAR1 activation is due to its thermoregulatory effects, but is also dose-dependent and dissipates at higher doses.

Acknowledgments

This research was generously funded by the Methamphetamine Abuse Research Center (P50 DA018165), National Institute of Health Institutional National Research Service Award (T32 NS007466), and the VA Merit Review and Research Career Scientist Programs (1I01BX002758).

The authors gratefully acknowledge David K. Grandy for providing *Taar1* transgenic breeders.

Abbreviations

5HT	serotonin
5HIAA	5-hydroxyindoleacetic acid
DA	dopamine
DAT	dopamine transporter
DOPAC	3,4-dihydroxyphenylacetic acid
EAAT2	excitatory amino acid transporter 2
ELISA	enzyme-linked immunosorbent assay
GFAP	glial fibrillary acidic protein
GLU	glutamate
GPCR	G-protein coupled receptor
HVA	homovanillic acid
MDMA	3,4-methylenedioxymethamphetamine
MA	methamphetamine

NET	norepinephrine transporter
NMDA	N-methyl-D-aspartate
PKA	protein kinase a
PKC	protein kinase c
ROS	reactive oxygen species
SERT	serotonin transporter
SNpc	substantia nigra pars compacta
TAAR1	trace-amine associated receptor 1
TH	tyrosine hydroxylase
VMAT2	vesicular monoamine transporter 2

References

- Achat-Mendes C, Lynch LJ, Sullivan KA, Vallender EJ, Miller GM. Augmentation of methamphetamine-induced behaviors in transgenic mice lacking the trace amine-associated receptor 1. *Pharmacol Biochem Behav.* 2012; 101:201–207. S0091-3057(11)00354-6 [pii]. DOI: 10.1016/j.pbb.2011.10.025 [PubMed: 22079347]
- Albers DS, Sonsalla PK. Methamphetamine-induced hyperthermia and dopaminergic neurotoxicity in mice: pharmacological profile of protective and nonprotective agents. *J Pharmacol Exp Ther.* 1995; 275:1104–1114. [PubMed: 8531070]
- Ali SF, Newport GD, Slikker W Jr. Methamphetamine-induced dopaminergic toxicity in mice. Role of environmental temperature and pharmacological agents. *Ann N Y Acad Sci.* 1996; 801:187–198. [PubMed: 8959033]
- Alvarsson A, Zhang X, Stan TL, Schintu N, Kadkhodaei B, Millan MJ, Perlmann T, Svenningsson P. Modulation by Trace Amine-Associated Receptor 1 of Experimental Parkinsonism, l-DOPA Responsivity, and Glutamatergic Neurotransmission. *J Neurosci.* 2015; 35:14057–14069. 35/41/14057 [pii]. DOI: 10.1523/JNEUROSCI.1312-15.2015 [PubMed: 26468205]
- Anderson CM, Swanson RA. Astrocyte glutamate transport: review of properties, regulation, and physiological functions. *Glia.* 2000; 32:1–14. DOI: 10.1002/1098-1136(200010)32:1<1::AID-GLIA10>3.0.CO;2-W [pii] [PubMed: 10975906]
- Anneken JH, Angoa-Perez M, Kuhn DM. 3,4-Methylenedioxypyrovalerone (MDPV) prevents while methylone enhances methamphetamine-induced damage to dopamine nerve endings: beta-ketoamphetamine modulation of neurotoxicity by the dopamine transporter. *J Neurochem.* 2015; doi: 10.1111/jnc.13048
- Ares-Santos S, Granado N, Espadas I, Martinez-Murillo R, Moratalla R. Methamphetamine causes degeneration of dopamine cell bodies and terminals of the nigrostriatal pathway evidenced by silver staining. *Neuropsychopharmacology.* 2014; 39:1066–1080. npp2013307 [pii]. DOI: 10.1038/npp.2013.307 [PubMed: 24169803]
- Borowsky B, Adham N, Jones KA, Raddatz R, Artymyshyn R, Ogozalek KL, Durkin MM, Lakhilani PP, Bonini JA, Pathirana S, Boyle N, Pu X, Kouranova E, Lichtblau H, Ochoa FY, Branchek TA, Gerald C. Trace amines: identification of a family of mammalian G protein-coupled receptors. *Proc Natl Acad Sci U S A.* 2001; 98:8966–8971. DOI: 10.1073/pnas.151105198;151105198 [pii] [PubMed: 11459929]
- Bove J, Perier C. Neurotoxin-based models of Parkinson's disease. *Neuroscience.* 2012; 211:51–76. S0306-4522(11)01266-8 [pii]. DOI: 10.1016/j.neuroscience.2011.10.057 [PubMed: 22108613]

- Bowyer JF, Davies DL, Schmued L, Broening HW, Newport GD, Slikker W Jr, Holson RR. Further studies of the role of hyperthermia in methamphetamine neurotoxicity. *J Pharmacol Exp Ther*. 1994; 268:1571–1580. [PubMed: 8138969]
- Bowyer JF, Hanig JP. Amphetamine- and methamphetamine-induced hyperthermia: Implications of the effects produced in brain vasculature and peripheral organs to forebrain neurotoxicity. *Temperature (Austin)*. 2014; 1:172–182. DOI: 10.4161/23328940.2014.982049;982049[pii] [PubMed: 27626044]
- Bowyer JF, Holson RR, Miller DB, O'Callaghan JP. Phenobarbital and dizocilpine can block methamphetamine-induced neurotoxicity in mice by mechanisms that are independent of thermoregulation. *Brain Res*. 2001; 919:179–183. S0006-8993(01)03051-7 [pii]. [PubMed: 11689178]
- Bradaia A, Trube G, Stalder H, Norcross RD, Ozmen L, Wettstein JG, Pinard A, Buchy D, Gassmann M, Hoener MC, Bettler B. The selective antagonist EPPTB reveals TAAR1-mediated regulatory mechanisms in dopaminergic neurons of the mesolimbic system. *Proc Natl Acad Sci U S A*. 2009; 106:20081–20086. 0906522106 [pii]. DOI: 10.1073/pnas.0906522106 [PubMed: 19892733]
- Broening HW, Morford LL, Vorhees CV. Interactions of dopamine D1 and D2 receptor antagonists with D-methamphetamine-induced hyperthermia and striatal dopamine and serotonin reductions. *Synapse*. 2005; 56:84–93. DOI: 10.1002/syn.20130 [PubMed: 15714503]
- Bunzow JR, Sonders MS, Arttamangkul S, Harrison LM, Zhang G, Quigley DI, Darland T, Suchland KL, Pasumamula S, Kennedy JL, Olson SB, Magenis RE, Amara SG, Grandy DK. Amphetamine, 3,4-methylenedioxymethamphetamine, lysergic acid diethylamide, and metabolites of the catecholamine neurotransmitters are agonists of a rat trace amine receptor. *Mol Pharmacol*. 2001; 60:1181–1188. [PubMed: 11723224]
- Burrows KB, Meshul CK. Methamphetamine alters presynaptic glutamate immunoreactivity in the caudate nucleus and motor cortex. *Synapse*. 1997; 27:133–144. DOI: 10.1002/(SICI)1098-2396(199710)27:2<133::AID-SYN4>3.0.CO;2-F [PubMed: 9266774]
- Center for Behavioral Health Statistics and Quality. [Last accessed: 6-6-2017] Behavioral health trends in the United States: Results from the 2014 National Survey on Drug Use and Health. 2015. <https://www.samhsa.gov/data/sites/default/files/NSDUH-FRR1-2014/NSDUH-FRR1-2014.pdf>
- Cubells JF, Rayport S, Rajendran G, Sulzer D. Methamphetamine neurotoxicity involves vacuolation of endocytic organelles and dopamine-dependent intracellular oxidative stress. *J Neurosci*. 1994; 14:2260–2271. [PubMed: 8158268]
- Darke S, Kaye S, McKetin R, Dufou J. Major physical and psychological harms of methamphetamine use. *Drug Alcohol Rev*. 2008; 27:253–262. 791758431 [pii]. DOI: 10.1080/09595230801923702 [PubMed: 18368606]
- Di Cara B, Maggio R, Aloisi G, Rivet JM, Lundius EG, Yoshitake T, Svenningsson P, Brocco M, Gobert A, De GL, Cistarelli L, Veiga S, De MC, Rodriguez M, Galizzi JP, Lockhart BP, Coge F, Boutin JA, Vayer P, Verdouw PM, Groenink L, Millan MJ. Genetic deletion of trace amine 1 receptors reveals their role in auto-inhibiting the actions of ecstasy (MDMA). *J Neurosci*. 2011; 31:16928–16940. 31/47/16928 [pii]. DOI: 10.1523/JNEUROSCI.2502-11.2011 [PubMed: 22114263]
- Docherty JR, Green AR. The role of monoamines in the changes in body temperature induced by 3,4-methylenedioxymethamphetamine (MDMA, ecstasy) and its derivatives. *Br J Pharmacol*. 2010; 160:1029–1044. BPH722 [pii]. DOI: 10.1111/j.1476-5381.2010.00722.x [PubMed: 20590597]
- Espinoza S, Ghisi V, Emanuele M, Leo D, Sukhanov I, Sotnikova TD, Chieregatti E, Gainetdinov RR. Postsynaptic D2 dopamine receptor supersensitivity in the striatum of mice lacking TAAR1. *Neuropharmacology*. 2015a; 93:308–313. S0028-3908(15)00057-X [pii]. DOI: 10.1016/j.neuropharm.2015.02.010 [PubMed: 25721394]
- Espinoza S, Lignani G, Caffino L, Maggi S, Sukhanov I, Leo D, Mus L, Emanuele M, Ronzitti G, Harmeier A, Medrihan L, Sotnikova TD, Chieregatti E, Hoener MC, Benfenati F, Tucci V, Fumagalli F, Gainetdinov RR. TAAR1 Modulates Cortical Glutamate NMDA Receptor Function. *Neuropsychopharmacology*. 2015b; npp201565 [pii]. doi: 10.1038/npp.2015.65
- Espinoza S, Salahpour A, Masri B, Sotnikova TD, Messa M, Barak LS, Caron MG, Gainetdinov RR. Functional interaction between trace amine-associated receptor 1 and dopamine D2 receptor. *Mol*

- Pharmacol. 2011; 80:416–425. mol.111.073304 [pii]. DOI: 10.1124/mol.111.073304 [PubMed: 21670104]
- Eyerman DJ, Yamamoto BK. A rapid oxidation and persistent decrease in the vesicular monoamine transporter 2 after methamphetamine. *J Neurochem.* 2007; 103:1219–1227. JNC4837 [pii]. DOI: 10.1111/j.1471-4159.2007.04837.x [PubMed: 17683483]
- Fantegrossi WE, Ciullo JR, Wakabayashi KT, De La, Garza R, Traynor JR, Woods JH. A comparison of the physiological, behavioral, neurochemical and microglial effects of methamphetamine and 3,4-methylenedioxymethamphetamine in the mouse. *Neuroscience.* 2008; 151:533–543. S0306-4522(07)01406-6 [pii]. DOI: 10.1016/j.neuroscience.2007.11.007 [PubMed: 18082974]
- Fleckenstein AE, Volz TJ, Riddle EL, Gibb JW, Hanson GR. New insights into the mechanism of action of amphetamines. *Annu Rev Pharmacol Toxicol.* 2007; 47:681–698. DOI: 10.1146/annurev.pharmtox.47.120505.105140 [PubMed: 17209801]
- Fukumura M, Cappon GD, Pu C, Broening HW, Vorhees CV. A single dose model of methamphetamine-induced neurotoxicity in rats: effects on neostriatal monoamines and glial fibrillary acidic protein. *Brain Res.* 1998; 806:1–7. S0006-8993(98)00656-8 [pii]. [PubMed: 9739098]
- Fumagalli F, Gainetdinov RR, Valenzano KJ, Caron MG. Role of dopamine transporter in methamphetamine-induced neurotoxicity: evidence from mice lacking the transporter. *J Neurosci.* 1998; 18:4861–4869. [PubMed: 9634552]
- Fumagalli F, Gainetdinov RR, Wang YM, Valenzano KJ, Miller GW, Caron MG. Increased methamphetamine neurotoxicity in heterozygous vesicular monoamine transporter 2 knock-out mice. *J Neurosci.* 1999; 19:2424–2431. [PubMed: 10087057]
- Glasner-Edwards S, Mooney LJ, Marinelli-Casey P, Hillhouse M, Ang A, Rawson RA. Psychopathology in methamphetamine-dependent adults 3 years after treatment. *Drug Alcohol Rev.* 2010; 29:12–20. DAR081 [pii]. DOI: 10.1111/j.1465-3362.2009.00081.x [PubMed: 20078677]
- Grace CE, Schaefer TL, Herring NR, Graham DL, Skelton MR, Gudelsky GA, Williams MT, Vorhees CV. Effect of a neurotoxic dose regimen of (+)-methamphetamine on behavior, plasma corticosterone, and brain monoamines in adult C57BL/6 mice. *Neurotoxicol Teratol.* 2010; 32:346–355. S0892-0362(10)00010-3 [pii]. DOI: 10.1016/j.ntt.2010.01.006 [PubMed: 20096350]
- Granado N, Ares-Santos S, O’Shea E, Vicario-Abejon C, Colado MI, Moratalla R. Selective vulnerability in striosomes and in the nigrostriatal dopaminergic pathway after methamphetamine administration: early loss of TH in striosomes after methamphetamine. *Neurotox Res.* 2010; 18:48–58. DOI: 10.1007/s12640-009-9106-1 [PubMed: 19760475]
- Granado N, Ares-Santos S, Oliva I, O’Shea E, Martin ED, Colado MI, Moratalla R. Dopamine D2-receptor knockout mice are protected against dopaminergic neurotoxicity induced by methamphetamine or MDMA. *Neurobiol Dis.* 2011; 42:391–403. S0969-9961(11)00054-4 [pii]. DOI: 10.1016/j.nbd.2011.01.033 [PubMed: 21303698]
- Guilarte TR, Nihei MK, McGlothlan JL, Howard AS. Methamphetamine-induced deficits of brain monoaminergic neuronal markers: distal axotomy or neuronal plasticity. *Neuroscience.* 2003; 122:499–513. S0306452203004767 [pii]. [PubMed: 14614914]
- Guillot TS, Shepherd KR, Richardson JR, Wang MZ, Li Y, Emson PC, Miller GW. Reduced vesicular storage of dopamine exacerbates methamphetamine-induced neurodegeneration and astrogliosis. *J Neurochem.* 2008; 106:2205–2217. JNC5568 [pii]. DOI: 10.1111/j.1471-4159.2008.05568.x [PubMed: 18643795]
- Hadlock GC, Chu PW, Walters ET, Hanson GR, Fleckenstein AE. Methamphetamine-induced dopamine transporter complex formation and dopaminergic deficits: the role of D2 receptor activation. *J Pharmacol Exp Ther.* 2010; 335:207–212. jpet.110.166660 [pii]. DOI: 10.1124/jpet.110.166660 [PubMed: 20622144]
- Hanson JE, Birdsall E, Seferian KS, Crosby MA, Keefe KA, Gibb JW, Hanson GR, Fleckenstein AE. Methamphetamine-induced dopaminergic deficits and refractoriness to subsequent treatment. *Eur J Pharmacol.* 2009; 607:68–73. [PubMed: 19326567]
- Harkness JH, Shi X, Janowsky A, Phillips TJ. Trace Amine-Associated Receptor 1 Regulation of Methamphetamine Intake and Related Traits. *Neuropsychopharmacology.* 2015; npp201561 [pii]. doi: 10.1038/npp.2015.61

- Harmeier A, Obermueller S, Meyer CA, Revel FG, Buchy D, Chaboz S, Dernick G, Wettstein JG, Iglesias A, Rolink A, Bettler B, Hoener MC. Trace amine-associated receptor 1 activation silences GSK3beta signaling of TAAR1 and D2R heteromers. *Eur Neuropsychopharmacol.* 2015; 25:2049–2061. S0924-977X(15)00264-3 [pii]. DOI: 10.1016/j.euroneuro.2015.08.011 [PubMed: 26372541]
- Hoffman WF, Moore M, Templin R, McFarland B, Hitzemann RJ, Mitchell SH. Neuropsychological function and delay discounting in methamphetamine-dependent individuals. *Psychopharmacology (Berl).* 2006; 188:162–170. DOI: 10.1007/s00213-006-0494-0 [PubMed: 16915378]
- Kita T, Miyazaki I, Asanuma M, Takeshima M, Wagner GC. Dopamine-induced behavioral changes and oxidative stress in methamphetamine-induced neurotoxicity. *Int Rev Neurobiol.* 2009; 88:43–64. S0074-7742(09)88003-3 [pii]. DOI: 10.1016/S0074-7742(09)88003-3 [PubMed: 19897074]
- Kiyatkin EA, Sharma HS. Acute methamphetamine intoxication: brain hyperthermia, blood-brain barrier, brain edema, and morphological cell abnormalities. *Int Rev Neurobiol.* 2009; 88:65–100. S0074-7742(09)88004-5 [pii]. DOI: 10.1016/S0074-7742(09)88004-5 [PubMed: 19897075]
- Krasnova IN, Cadet JL. Methamphetamine toxicity and messengers of death. *Brain Res Rev.* 2009; 60:379–407. S0165-0173(09)00034-4 [pii]. DOI: 10.1016/j.brainresrev.2009.03.002 [PubMed: 19328213]
- Kuhn DM, Angoa-Perez M, Thomas DM. Nucleus accumbens invulnerability to methamphetamine neurotoxicity. *ILAR J.* 2011; 52:352–365. ilar.52.3.352 [pii]. DOI: 10.1093/ilar.52.3.352 [PubMed: 23382149]
- Ladenheim B, Krasnova IN, Deng X, Oyler JM, Poletini A, Moran TH, Huestis MA, Cadet JL. Methamphetamine-induced neurotoxicity is attenuated in transgenic mice with a null mutation for interleukin-6. *Mol Pharmacol.* 2000; 58:1247–1256. [PubMed: 11093760]
- Lau JW, Senok S, Stadlin A. Methamphetamine-induced oxidative stress in cultured mouse astrocytes. *Ann N Y Acad Sci.* 2000; 914:146–156. [PubMed: 11085317]
- LaVoie MJ, Card JP, Hastings TG. Microglial activation precedes dopamine terminal pathology in methamphetamine-induced neurotoxicity. *Exp Neurol.* 2004; 187:47–57. DOI: 10.1016/j.expneurol.2004.01.010;S0014488604000202 [pii] [PubMed: 15081587]
- LaVoie MJ, Hastings TG. Dopamine quinone formation and protein modification associated with the striatal neurotoxicity of methamphetamine: evidence against a role for extracellular dopamine. *J Neurosci.* 1999; 19:1484–1491. [PubMed: 9952424]
- Leo D, Mus L, Espinoza S, Hoener MC, Sotnikova TD, Gainetdinov RR. Taar1-mediated modulation of presynaptic dopaminergic neurotransmission: role of D2 dopamine autoreceptors. *Neuropharmacology.* 2014; 81:283–291. S0028-3908(14)00071-9 [pii]. DOI: 10.1016/j.neuropharm.2014.02.007 [PubMed: 24565640]
- Lindemann L, Meyer CA, Jeanneau K, Bradaia A, Ozmen L, Bluethmann H, Bettler B, Wettstein JG, Borroni E, Moreau JL, Hoener MC. Trace amine-associated receptor 1 modulates dopaminergic activity. *J Pharmacol Exp Ther.* 2008; 324:948–956. jpet.107.132647 [pii]. DOI: 10.1124/jpet.107.132647 [PubMed: 18083911]
- Matsumoto RR, Seminerio MJ, Turner RC, Robson MJ, Nguyen L, Miller DB, O'Callaghan JP. Methamphetamine-induced toxicity: an updated review on issues related to hyperthermia. *Pharmacol Ther.* 2014; 144:28–40. S0163-7258(14)00096-5 [pii]. DOI: 10.1016/j.pharmthera.2014.05.001 [PubMed: 24836729]
- McConnell SE, O'Banion MK, Cory-Slechta DA, Olschowka JA, Opanashuk LA. Characterization of binge-dosed methamphetamine-induced neurotoxicity and neuroinflammation. *Neurotoxicology.* 2015; 50:131–141. S0161-813X(15)00121-7 [pii]. DOI: 10.1016/j.neuro.2015.08.006 [PubMed: 26283213]
- McKetin R, McLaren J, Lubman DI, Hides L. The prevalence of psychotic symptoms among methamphetamine users. *Addiction.* 2006; 101:1473–1478. ADD1496 [pii]. DOI: 10.1111/j.1360-0443.2006.01496.x [PubMed: 16968349]
- Metzger RR, Haughey HM, Wilkins DG, Gibb JW, Hanson GR, Fleckenstein AE. Methamphetamine-induced rapid decrease in dopamine transporter function: role of dopamine and hyperthermia. *J Pharmacol Exp Ther.* 2000; 295:1077–1085. [PubMed: 11082443]

- Miller DB, O'Callaghan JP. Environment-, drug- and stress-induced alterations in body temperature affect the neurotoxicity of substituted amphetamines in the C57BL/6J mouse. *J Pharmacol Exp Ther.* 1994; 270:752–760. [PubMed: 8071868]
- Miller DB, O'Callaghan JP. Elevated environmental temperature and methamphetamine neurotoxicity. *Environ Res.* 2003; 92:48–53. S0013935102000518 [pii]. [PubMed: 12706754]
- Miner NB, O'Callaghan JP, Phillips TJ, Janowsky A. The combined effects of 3,4-methylenedioxymethamphetamine (MDMA) and selected substituted methcathinones on measures of neurotoxicity. *Neurotoxicol Teratol.* 2017; S0892-0362(16)30134-9 [pii]. doi: 10.1016/j.ntt.2017.02.003
- Mooney LJ, Glasner-Edwards S, Marinelli-Casey P, Hillhouse M, Ang A, Hunter J, Haning W, Colescott P, Ling W, Rawson R. Health conditions in methamphetamine-dependent adults 3 years after treatment. *J Addict Med.* 2009; 3:155–163. DOI: 10.1097/ADM.0b013e3181a17c79;01271255-200909000-00007[pii] [PubMed: 21769012]
- Morgan ME, Gibb JW. Short-term and long-term effects of methamphetamine on biogenic amine metabolism in extra-striatal dopaminergic nuclei. *Neuropharmacology.* 1980; 19:989–995. [PubMed: 6106905]
- Myles BJ, Jarrett LA, Broom SL, Speaker HA, Sabol KE. The effects of methamphetamine on core body temperature in the rat--part 1: chronic treatment and ambient temperature. *Psychopharmacology (Berl).* 2008; 198:301–311. DOI: 10.1007/s00213-007-1061-z [PubMed: 18438646]
- O'Callaghan JP. Measurement of glial fibrillary acidic protein. *Curr Protoc Toxicol.* 2002; Chapter 12(Unit12)doi: 10.1002/0471140856.tx1208s11
- O'Callaghan JP, Kelly KA, VanGilder RL, Sofroniew MV, Miller DB. Early Activation of STAT3 Regulates Reactive Astroglia Induced by Diverse Forms of Neurotoxicity. *PLoS One.* 2014; 9:e102003.doi: 10.1371/journal.pone.0102003;PONE-D-14-12852[pii] [PubMed: 25025494]
- O'Callaghan JP, Miller DB. Neurotoxicity profiles of substituted amphetamines in the C57BL/6J mouse. *J Pharmacol Exp Ther.* 1994; 270:741–751. [PubMed: 8071867]
- O'Callaghan JP, Sriram K. Glial fibrillary acidic protein and related glial proteins as biomarkers of neurotoxicity. *Expert Opin Drug Saf.* 2005; 4:433–442. DOI: 10.1517/14740338.4.3.433 [PubMed: 15934851]
- Panas MW, Xie Z, Panas HN, Hoener MC, Vallender EJ, Miller GM. Trace amine associated receptor 1 signaling in activated lymphocytes. *J Neuroimmune Pharmacol.* 2012; 7:866–876. DOI: 10.1007/s11481-011-9321-4 [PubMed: 22038157]
- Pu C, Vorhees CV. Developmental dissociation of methamphetamine-induced depletion of dopaminergic terminals and astrocyte reaction in rat striatum. *Brain Res Dev Brain Res.* 1993; 72:325–328. [PubMed: 8097974]
- Revel FG, Moreau JL, Gainetdinov RR, Bradaia A, Sotnikova TD, Mory R, Durkin S, Zbinden KG, Norcross R, Meyer CA, Metzler V, Chaboz S, Ozmen L, Trube G, Pouzet B, Bettler B, Caron MG, Wettstein JG, Hoener MC. TAAR1 activation modulates monoaminergic neurotransmission, preventing hyperdopaminergic and hypoglutamatergic activity. *Proc Natl Acad Sci U S A.* 2011; 108:8485–8490. 1103029108 [pii]. DOI: 10.1073/pnas.1103029108 [PubMed: 21525407]
- Revel FG, Moreau JL, Pouzet B, Mory R, Bradaia A, Buchy D, Metzler V, Chaboz S, Groebke ZK, Galley G, Norcross RD, Tuerck D, Bruns A, Morairty SR, Kilduff TS, Wallace TL, Risterucci C, Wettstein JG, Hoener MC. A new perspective for schizophrenia: TAAR1 agonists reveal antipsychotic- and antidepressant-like activity, improve cognition and control body weight. *Mol Psychiatry.* 2013; 18:543–556. mp201257 [pii]. DOI: 10.1038/mp.2012.57 [PubMed: 22641180]
- Scott JC, Woods SP, Matt GE, Meyer RA, Heaton RK, Atkinson JH, Grant I. Neurocognitive effects of methamphetamine: a critical review and meta-analysis. *Neuropsychol Rev.* 2007; 17:275–297. DOI: 10.1007/s11065-007-9031-0 [PubMed: 17694436]
- Seeman P, Weinshenker D, Quirion R, Srivastava LK, Bhardwaj SK, Grandy DK, Premont RT, Sotnikova TD, Boksa P, El-Ghundi M, O'dowd BF, George SR, Perreault ML, Mannisto PT, Robinson S, Palmiter RD, Tallero T. Dopamine supersensitivity correlates with D2High states, implying many paths to psychosis. *Proc Natl Acad Sci U S A.* 2005; 102:3513–3518. 0409766102 [pii]. DOI: 10.1073/pnas.0409766102 [PubMed: 15716360]

- Shabani S, Houlton SK, Hellmuth L, Mojica E, Mootz JR, Zhu Z, Reed C, Phillips TJ. A Mouse Model for Binge-Level Methamphetamine Use. *Front Neurosci.* 2016; 10:493. doi: 10.3389/fnins.2016.00493 [PubMed: 27853417]
- Shabani S, McKinnon CS, Cunningham CL, Phillips TJ. Profound reduction in sensitivity to the aversive effects of methamphetamine in mice bred for high methamphetamine intake. *Neuropharmacology.* 2012; 62:1134–1141. S0028-3908(11)00484-9 [pii]. DOI: 10.1016/j.neuropharm.2011.11.005 [PubMed: 22118879]
- Sharma HS, Kiyatkin EA, Patnaik R, Lafuente JV, Muresanu DF, Sjoquist PO, Sharma A. Exacerbation of Methamphetamine Neurotoxicity in Cold and Hot Environments: Neuroprotective Effects of an Antioxidant Compound H-290/51. *Mol Neurobiol.* 2015; 52:1023–1033. DOI: 10.1007/s12035-015-9252-9 [pii] [PubMed: 26111626]
- Shi X, Walter NA, Harkness JH, Neve KA, Williams RW, Lu L, Belknap JK, Eshleman AJ, Phillips TJ, Janowsky A. Genetic Polymorphisms Affect Mouse and Human Trace Amine-Associated Receptor 1 Function. *PLoS One.* 2016; 11:e0152581. [doi];PONE-D-15-52839 [pii]. doi: 10.1371/journal.pone.0152581 [PubMed: 27031617]
- Shortall SE, Green AR, Swift KM, Fone KC, King MV. Differential effects of cathinone compounds and MDMA on body temperature in the rat, and pharmacological characterization of mephedrone-induced hypothermia. *Br J Pharmacol.* 2013; 168:966–977. DOI: 10.1111/j.1476-5381.2012.02236.x [PubMed: 23043631]
- Shuto T, Seeman P, Kuroiwa M, Nishi A. Repeated administration of a dopamine D1 receptor agonist reverses the increased proportions of striatal dopamine D1^{High} and D2^{High} receptors in methamphetamine-sensitized rats. *Eur J Neurosci.* 2008; 27:2551–2557. EJN6221 [pii]. DOI: 10.1111/j.1460-9568.2008.06221.x [PubMed: 18489579]
- Siemian JN, Zhang Y, Li JX. Trace amine-associated receptor 1 agonists RO5263397 and RO5166017 attenuate quinpirole-induced yawning but not hypothermia in rats. *Behav Pharmacol.* 2017; doi: 10.1097/FBP.0000000000000330
- Simon SL, Domier C, Carnell J, Brethen P, Rawson R, Ling W. Cognitive impairment in individuals currently using methamphetamine. *Am J Addict.* 2000; 9:222–231. [PubMed: 11000918]
- Sonsalla PK, Jochnowitz ND, Zeevalk GD, Oostveen JA, Hall ED. Treatment of mice with methamphetamine produces cell loss in the substantia nigra. *Brain Res.* 1996; 738:172–175. 0006-8993(96)00995-X [pii]. [PubMed: 8949944]
- Sonsalla PK, Nicklas WJ, Heikkila RE. Role for excitatory amino acids in methamphetamine-induced nigrostriatal dopaminergic toxicity. *Science.* 1989; 243:398–400. [PubMed: 2563176]
- Sotnikova TD, Zorina OI, Ghisi V, Caron MG, Gainetdinov RR. Trace amine associated receptor 1 and movement control. *Parkinsonism Relat Disord.* 2008; 14(Suppl 2):S99–102. S1353-8020(08)00120-X [pii]. DOI: 10.1016/j.parkreldis.2008.04.006 [PubMed: 18585080]
- Sriram K, Benkovic SA, Hebert MA, Miller DB, O'Callaghan JP. Induction of gp130-related cytokines and activation of JAK2/STAT3 pathway in astrocytes precedes up-regulation of glial fibrillary acidic protein in the 1-methyl-4-phenyl-1,2,3,6-tetrahydropyridine model of neurodegeneration: key signaling pathway for astrogliosis in vivo? *J Biol Chem.* 2004; 279:19936–19947. DOI: 10.1074/jbc.M309304200;M309304200 [pii] [PubMed: 14996842]
- Substance Abuse and Mental Health Services Administration. [Last accessed: 6-6-2017] The DAWN Report: Emergency Department Visits Involving Methamphetamine: 2007 to 2011. 2014. https://www.samhsa.gov/data/sites/default/files/DAWN_SR167_EDVisitsMeth_06-12-14/DAWN-SR167-EDVisitsMeth-2014.htm
- Sukhanov I, Caffino L, Efimova EV, Espinoza S, Sotnikova TD, Cervo L, Fumagalli F, Gainetdinov RR. Increased context-dependent conditioning to amphetamine in mice lacking TAAR1. *Pharmacol Res.* 2016; 103:206–214. S1043-6618(15)00263-7 [pii]. DOI: 10.1016/j.phrs.2015.11.002 [PubMed: 26640076]
- Thomas DM, Dowgiert J, Geddes TJ, Francescutti-Verbeem D, Liu X, Kuhn DM. Microglial activation is a pharmacologically specific marker for the neurotoxic amphetamines. *Neurosci Lett.* 2004; 367:349–354. S0304-3940(04)00767-0 [pii]. DOI: 10.1016/j.neulet.2004.06.065 [PubMed: 15337264]
- United Nations Office on Drugs and Crime. [Last accessed: 6-6-2017] World Drug Report 2016. 2016. <http://www.unodc.org/doc/wdr2016>

- Volkow ND, Chang L, Wang GJ, Fowler JS, Leonido-Yee M, Franceschi D, Sedler MJ, Gatley SJ, Hitzemann R, Ding YS, Logan J, Wong C, Miller EN. Association of dopamine transporter reduction with psychomotor impairment in methamphetamine abusers. *Am J Psychiatry*. 2001; 158:377–382. DOI: 10.1176/appi.ajp.158.3.377 [PubMed: 11229977]
- Wheeler JM, Reed C, Burkhart-Kasch S, Li N, Cunningham CL, Janowsky A, Franken FH, Wren KM, Hashimoto JG, Scibelli AC, Phillips TJ. Genetically correlated effects of selective breeding for high and low methamphetamine consumption. *Genes Brain Behav*. 2009; 8:758–771. GBB522 [pii]. DOI: 10.1111/j.1601-183X.2009.00522.x [PubMed: 19689456]
- Wilson JM, Kalasinsky KS, Levey AI, Bergeron C, Reiber G, Anthony RM, Schmunk GA, Shannak K, Haycock JW, Kish SJ. Striatal dopamine nerve terminal markers in human, chronic methamphetamine users. *Nat Med*. 1996; 2:699–703. [PubMed: 8640565]
- Wolinsky TD, Swanson CJ, Smith KE, Zhong H, Borowsky B, Seeman P, Branchek T, Gerald CP. The Trace Amine 1 receptor knockout mouse: an animal model with relevance to schizophrenia. *Genes Brain Behav*. 2007; 6:628–639. GBB292 [pii]. DOI: 10.1111/j.1601-183X.2006.00292.x [PubMed: 17212650]
- Xu W, Zhu JP, Angulo JA. Induction of striatal pre- and postsynaptic damage by methamphetamine requires the dopamine receptors. *Synapse*. 2005; 58:110–121. DOI: 10.1002/syn.20185 [PubMed: 16088948]
- Yamamoto BK, Raudensky J. The role of oxidative stress, metabolic compromise, and inflammation in neuronal injury produced by amphetamine-related drugs of abuse. *J Neuroimmune Pharmacol*. 2008; 3:203–217. DOI: 10.1007/s11481-008-9121-7 [PubMed: 18709468]
- Zhang L, Shirayama Y, Shimizu E, Iyo M, Hashimoto K. Protective effects of minocycline on 3,4-methylenedioxymethamphetamine-induced neurotoxicity in serotonergic and dopaminergic neurons of mouse brain. *Eur J Pharmacol*. 2006; 544:1–9. S0014-2999(06)00541-3 [pii]. DOI: 10.1016/j.ejphar.2006.05.047 [PubMed: 16859675]
- Zhu JP, Xu W, Angulo N, Angulo JA. Methamphetamine-induced striatal apoptosis in the mouse brain: comparison of a binge to an acute bolus drug administration. *Neurotoxicology*. 2006; 27:131–136. S0161-813X(05)00095-1 [pii]. DOI: 10.1016/j.neuro.2005.05.014 [PubMed: 16165214]

Highlight

- TAAR1 knockout mouse model used to investigate receptor's role in MA neurotoxicity.
- TAAR1 activation diminishes MA neurotoxicity.
- TAAR1 activation potentiates acute hypothermic response to MA.
- TAAR1 regulatory effects are dose-dependent and disappear at highest dose of MA.
- Neuroprotection provided by TAAR1 activation attributed to thermoregulatory effect.

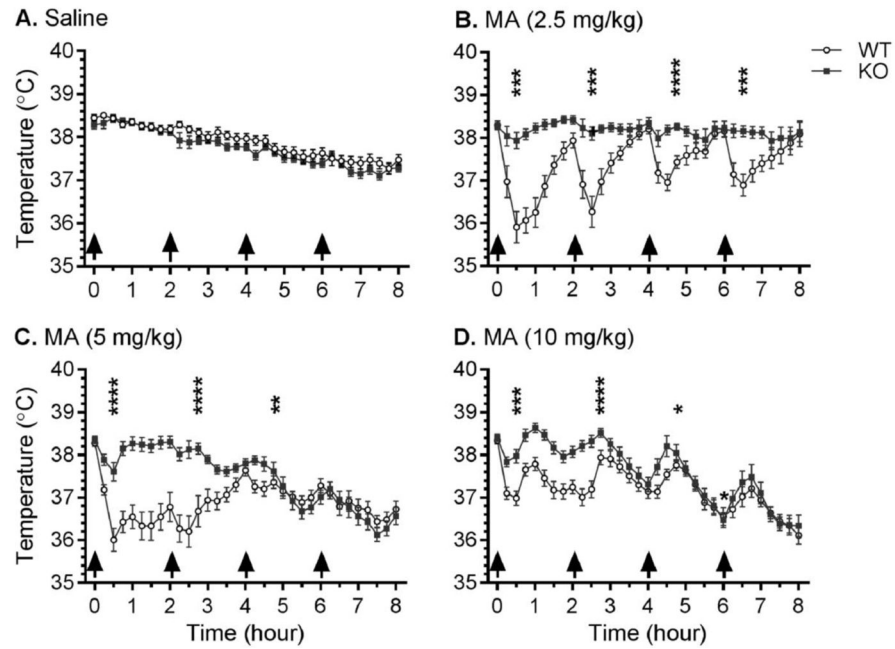


Figure 1.

Effects of repeated saline or MA injections on core body temperature. *Taar1*-WT and -KO mice received 4 i.p. injections (indicated by arrows) of saline or MA (2.5, 5, or 10 mg/kg), spaced 2 hr apart. Body temperature was measured every 15 min *via* telemetry over 8 hr in an ambient temperature of $23 \pm 1^\circ\text{C}$. Data represent temperature for each genotype and treatment group (mean \pm SEM) at specified time points, $n = 11\text{--}21$ mice per group. Time points selected for detailed analysis were 30 min after each injection. *: $p < 0.05$, **: $p < 0.01$, ***: $p < 0.001$, ****: $p < 0.0001$ compared between genotypes.

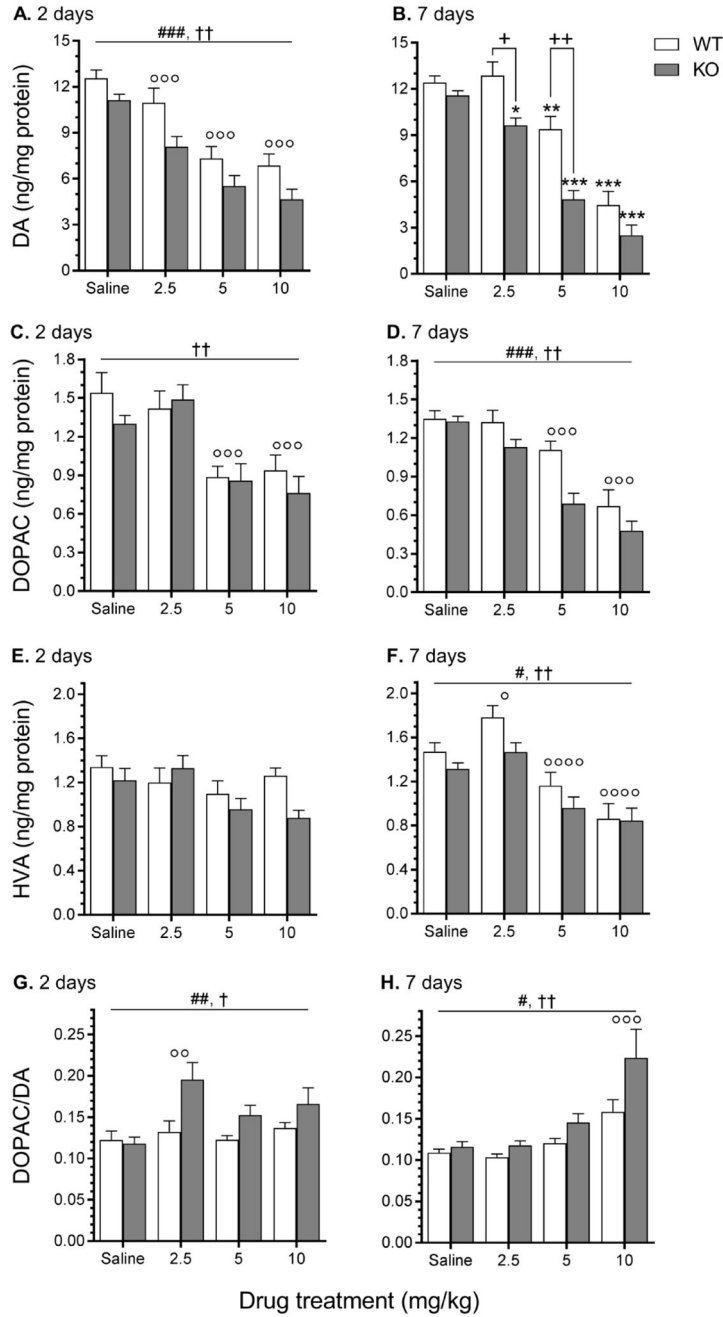


Figure 2. Striatal levels of DA, DOPAC, HVA and DA turnover measured 2 and 7 days following saline or MA treatment. *Taar1*-WT and -KO mice received 4 i.p. injections of saline or MA (2.5, 5, or 10 mg/kg), spaced 2 hr apart and were euthanized either 2 or 7 days following the final injection for striatal tissue collection. Values were normalized to the amount of protein in each tissue sample. Data represent means \pm SEM of 7–11 mice per group. *: $p < 0.05$, **: $p < 0.01$, ***: $p < 0.001$ compared to saline-treated controls; +: $p < 0.001$, ++: $p < 0.0001$ between genotypes; #: $p < 0.05$, ##: $p < 0.01$, ###: $p < 0.001$ for main effect of genotype; †: $p < 0.05$, ††: $p < 0.01$, †††: $p < 0.001$ for main effect of genotype; †: $p < 0.05$, ††: $p < 0.01$, †††: $p < 0.001$ for main effect of genotype; †: $p < 0.05$, ††: $p < 0.01$, †††: $p < 0.001$ for main effect of genotype; †: $p < 0.05$, ††: $p < 0.01$, †††: $p < 0.001$ for main effect of genotype; †: $p < 0.05$, ††: $p < 0.01$, †††: $p < 0.001$ for main effect of genotype.

$p < 0.01$, ††: $p < 0.0001$ for main effect of dose; °: $p < 0.05$, °°: $p < 0.01$, °°°: $p < 0.001$, °°°°:
 $p < 0.0001$ compared to saline-treated controls, regardless of genotype.

Author Manuscript

Author Manuscript

Author Manuscript

Author Manuscript

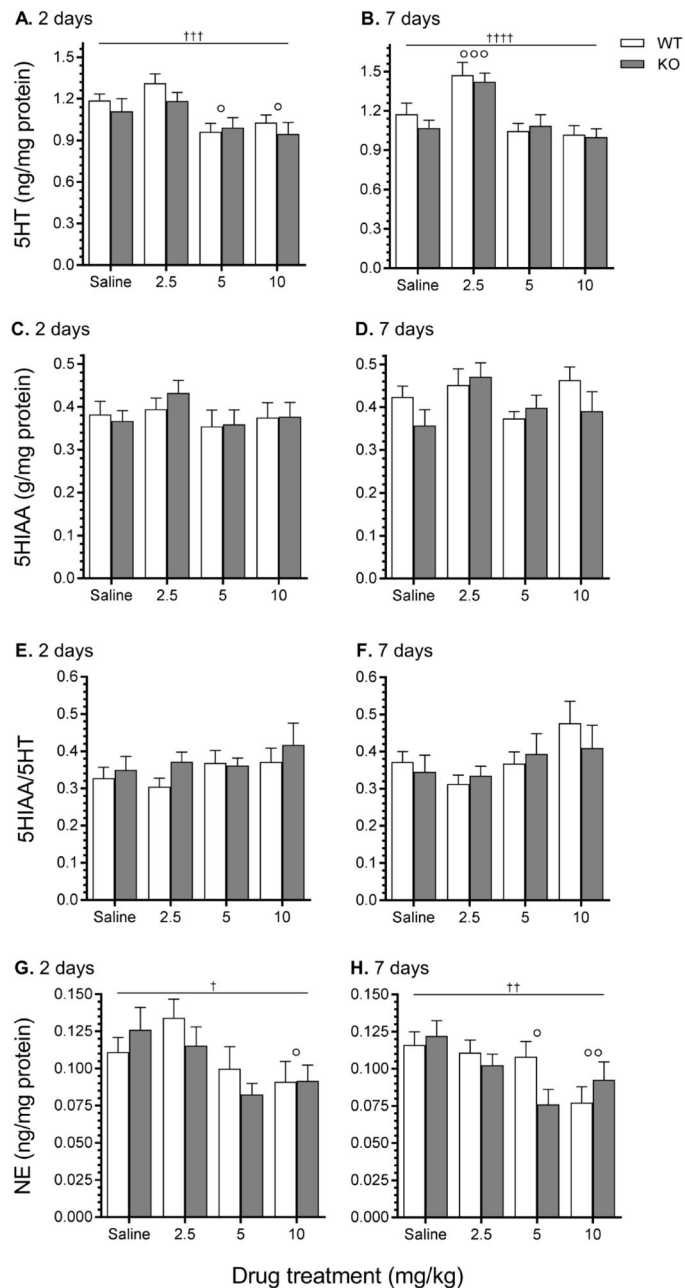


Figure 3.

Striatal levels of 5HT, 5HIAA, 5HT turnover, and NE measured 2 and 7 days following saline or MA treatment. *Taar1*-WT and -KO mice received 4 i.p. injections of saline or MA (2.5, 5, or 10 mg/kg), spaced 2 hr apart and were euthanized either 2 or 7 days following the final injection for striatal tissue collection. Values were normalized to the amount of protein in each tissue sample. Data represent means \pm SEM of 7–11 mice per group. †: $p < 0.05$, ††: $p < 0.01$, †††: $p < 0.001$, ††††: $p < 0.0001$ for main effect of dose; °: $p < 0.05$, °°: $p < 0.01$, °°°: $p < 0.001$ compared to saline-treated controls, regardless of genotype.

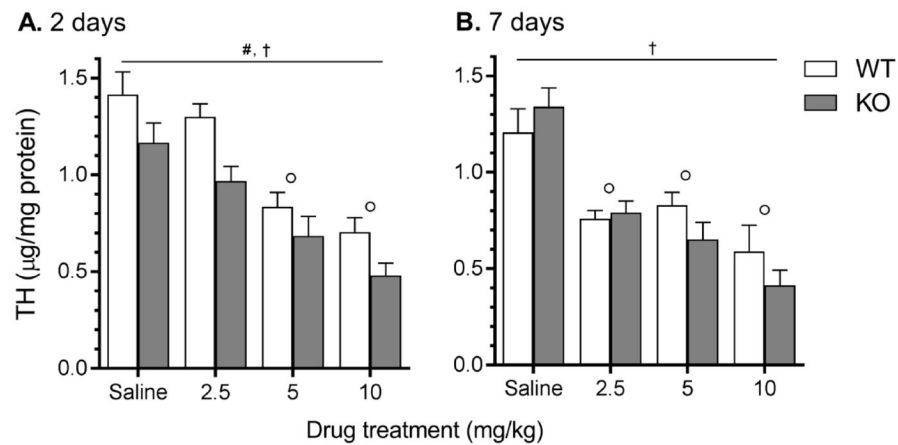


Figure 4.

Striatal TH levels measured *via* sandwich ELISA 2 and 7 days following saline or MA treatment. *Taar1*-WT and -KO mice received 4 i.p. injections of saline or MA (2.5, 5, or 10 mg/kg), spaced 2 hr apart. Animals were euthanized either 2 (A.) or 7 (B.) days following the final injection for striatal tissue collection. TH values were normalized to the amount of protein in each tissue sample. Data represent means \pm SEM of 7–11 mice per group. #: $p < 0.001$ for main effect of genotype, †: $p < 0.0001$ for main effect of dose; ∘: $p < 0.001$ compared to saline-treated controls, regardless of genotype.

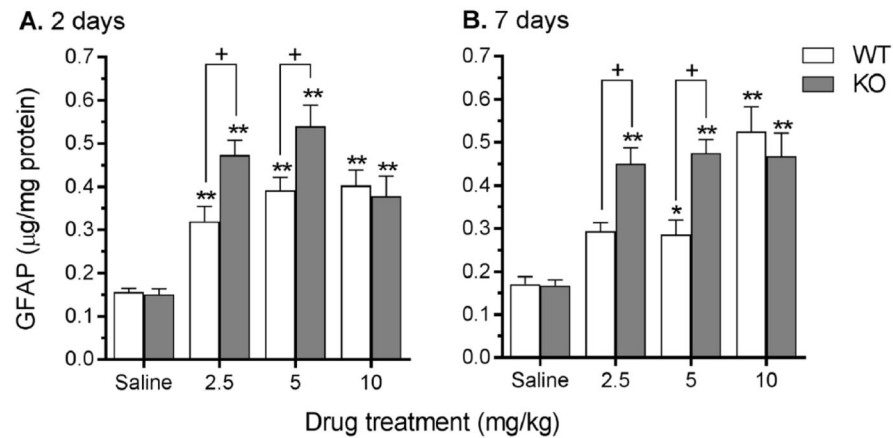


Figure 5.

Striatal GFAP levels measured *via* sandwich ELISA 2 and 7 days following saline or MA treatment. *Taar1*-WT and -KO mice received 4 i.p. injections of saline or MA (2.5, 5, or 10 mg/kg), spaced 2 hr apart. Animals were euthanized either 2 (A.) or 7 (B.) days following the final injection for striatal tissue collection. GFAP values were normalized to the amount of protein in each tissue sample. Data represent means \pm SEM of 7–11 mice per group. *: $p < 0.05$, **: $p < 0.001$ compared to saline-treated controls; +: $p < 0.001$ between genotypes.

Table 1

MA-induced change in temperature relative to saline-treated mice.

<i>Taar1</i>	MA (mg/kg)	30 min post-injection (°C ± SEM)			
		1st Inj	2nd Inj	3rd Inj	4th Inj
WT	2.5	-2.53 ± 0.37 ^c	-1.91 ± 0.36 ^c	-0.96 ± 0.19 ^b	-0.56 ± 0.26
	5	-2.44 ± 0.27 ^c	-1.98 ± 0.36 ^c	-0.71 ± 0.17 ^a	-0.65 ± 0.22
	10	-1.45 ± 0.17 ^c	-0.99 ± 0.20 ^b	-0.37 ± 0.12	-0.43 ± 0.24
KO	2.5	-0.50 ± 0.20	0.22 ± 0.16	0.40 ± 0.11	0.78 ± 0.13 ^b
	5	-0.83 ± 0.22 ^a	0.24 ± 0.21	0.01 ± 0.17	-0.44 ± 0.21
	10	-0.47 ± 0.16 ^a	0.44 ± 0.14	0.42 ± 0.25	-0.02 ± 0.26

Data represent change in temperature (mean ± SEM) for each treatment group from saline- treated mice at specified time point, *n* = 11–21 mice per group.

^a *p* < 0.05;

^b *p* < 0.01;

^c *p* < 0.001 in analysis compared to saline-treated controls.